Role of Encapsulated Metal Cation in the Reactivity and Regioselectivity of the C 60 Diels–Alder Reaction

ARTICLE *in* THE JOURNAL OF PHYSICAL CHEMISTRY A · FEBRUARY 2015

Impact Factor: 2.69 · DOI: 10.1021/acs.jpca.5b00194 · Source: PubMed

2 AUTHORS, INCLUDING:

Cui Chengxing
Beijing Normal University
10 PUBLICATIONS **24** CITATIONS

THE JOURNAL OF PHYSICAL CHEMISTRY A

Article

pubs.acs.org/JPCA

Role of Encapsulated Metal Cation in the Reactivity and Regioselectivity of the C_{60} Diels–Alder Reaction

Cheng-Xing Cui[†,‡] and Ya-Jun Liu*[,†]

[†]College of Chemistry, Key Laboratory of Theoretical and Computational Photochemistry, Ministry of Education, Beijing Normal University, Beijing 100875, China

[‡]School of Chemistry and Chemical Engineering, Henan Institute of Science and Technology, Xinxiang 453003, China

Supporting Information

ABSTRACT: Endohedral metallofullerene has novel properties because of the interaction between the encapsulated metal atom or cation and fullerene. Experiments have demonstrated that the insertion of Li^+ into C_{60} can greatly promote the reactivity of the Diels–Alder (DA) cycloaddition of cyclopentadiene (CpH) to C_{60}. However, the reaction is sufficiently fast that its quantitative kinetic data cannot be obtained experimentally. In addition, knowledge regarding the effects of other alkali metal cations and metal cations with more charges on the reactivity and regioselectivity of C_{60} is almost nonexistent. In the current study, DA cycloadditions of CpH to $M^+@C_{60}$ (where M = Li, Na, K, Rb, and Cs) and $Ca^{2+}@C_{60}$ were investigated via density functional theory in the gas phase and in solvent. Via careful discussion and comparison with the results of C_{60}, we concluded the following for the DA reaction of CpH to C_{60} and, more generally, for DA reactions of other fullerenes: (1) the encapsulated metal cations enhance the reactivity; (2) among alkali metal cations, Na^+ could be the best catalyst; (3) Ca^{2+} is more favorable in promoting the reactivity than any alkali metal cation; (4) encapsulated metal cations with more positive charges enhance the reactivity of the 6–5 bond in C_{60}, which is significant when the 6–5 adduct is the target product.

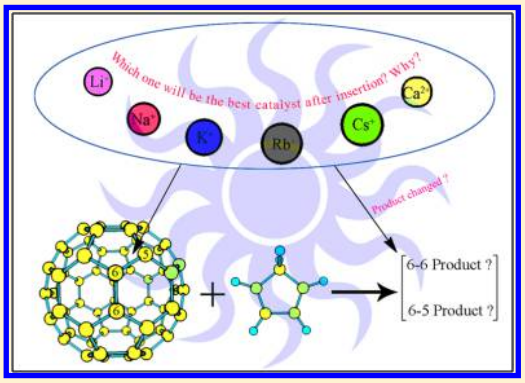

1. INTRODUCTION

Endohedral metallofullerenes (EMFs) have the potential to prepare interesting electronic materials, such as superconductors, because they are less sensitive to air than alkali metal intercalated fullerene materials.[1−4] Although C_{60} is the most abundant fullerene, the mono-metal-encapsulated C_{60} ($M@C_{60}$) was not isolated for a long time because $M@C_{60}$ is not soluble in standard solvents used for fullerene extraction.[5,6] This dilemma was solved by using aniline and pyridine as solvents. $Ca@C_{60}$ and several lanthanide-metal-encapsulated C_{60} compounds were successfully extracted by the two solvents.[7,8] Then, via self-propagating high-temperature synthesis, the encapsulations of K, Rb, Ba, and Ca into C_{60} were demonstrated;[9,10] among them, K- and Ca-doped C_{60} have been shown to be superconductive at 18 K.[9,11] C_{60} doped with the group I metals (Li, Na, K, Rb, and Cs) have attracted considerable attention because they are conductive.[12] Tellgmann et al. efficiently prepared $Li@C_{60}$ in macroscopic amounts by repeatedly exposing monolayers of C_{60} to an intense Li^+ beam.[2] Another form of encapsulated C_{60}, the polar cationic form of lithium-encapsulated C_{60} ($Li^+@C_{60}$), was synthesized in pure form and structurally characterized, and its optical properties were then investigated.[3,13] As the only reported endohedral metal cation fullerene (EMCF) to date, $Li^+@C_{60}$ has been suggested to be useful as an indispensable unit in functionalized nanoscale materials in organic electronics and medicinal chemistry[14−16] because its reactivity in photoinduced electron-transfer reduction with electron donors is greatly enhanced compared to that of empty C_{60}.[17] The addition patterns of EMFs are different from those of empty fullerenes.[6,18] The group of Matsuo experimentally examined the DA cycloaddition of 1,3-cyclopentadiene (CpH) to $Li^+@C_{60}$ and successfully isolated and structurally characterized the CpH monoadduct of $Li^+@C_{60}$.[19] Recently, the same group studied the kinetics of the DA cycloaddition of 1,3-cyclohexadiene to $Li^+@C_{60}$ and characterized the obtained product.[20] They concluded that DA cycloadditions of CpH and 1,3-cyclohexadiene to the 6–6 bond of $Li^+@C_{60}$ were 1000- and 2700-fold faster than the corresponding additions to the 6–6 bond of empty C_{60}, respectively.[19,20] These two contributions deserve a thorough investigation to uncover how the DA reactions of cyclodienes and C_{60} are affected by the encapsulated Li^+.

Theoretical methods are an indispensable tool for probing the properties of novel materials and understanding new chemical reactions. The properties of $M^+@C_{60}$ (M represents H, Li, Na, and K) were theoretically investigated by density function theory (DFT).[21] In an experimental study on the DA cycloaddition of 1,3-cyclohexadiene to $Li^+@C_{60}$, Ueno explained the enhanced DA cycloaddition rate using DFT.[20] The kinetics of the very fast

Received: January 8, 2015
Revised: February 14, 2015
Published: February 25, 2015

DOI: 10.1021/acs.jpca.5b00194
J. Phys. Chem. A 2015, 119, 3098−3106

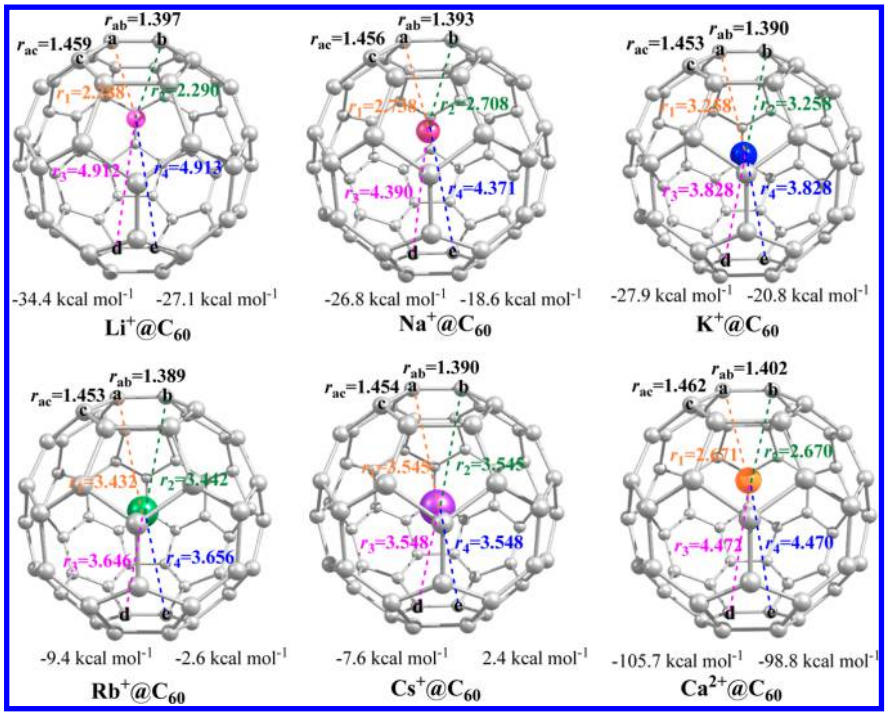

Figure 1. Dominant geometric parameters (in Å) and the interaction energy (kcal mol^{-1}) in enthalpy (the left one) and Gibbs energy (the right one) of $M^+@C_{60}$ calculated at the M06-2X/6-31G(d,p) level.

DA cycloaddition of CpH to $Li^+@C_{60}$ are difficult to investigate experimentally, and there is no available computational data.[19] Thus, due to the deficiency of experimental and theoretical information, the effect of encapsulated Li^+ on the reactivity and regioselectivity of C_{60} cannot be uncovered. The effects of four other alkali metal cations (Na^+, K^+, Rb^+, and Cs^+) on the DA cycloaddition of CpH to C_{60} also remain unknown. Moreover, the effects of encapsulated cations with more charge have not been probed either. In this paper, the effects of encapsulated metal cations on this DA reaction were systematically investigated via DFT. The M06-2X functional has been suggested for use in fields concerning main group thermochemistry, kinetics, and noncovalent interactions such as van der Waals interactions.[22] This functional can give accurate thermodynamics for C−C bond-forming reactions[23] and has been demonstrated to yield reasonable energetics for DA reactions and 1,3-dipolar cycloaddition reactions.[24−26] Using this functional, we have systematically investigated the DA reaction between 1,3-butadiene and ethylene along with the regioselectivity and substituent effects of cycloaddition reactions of C_{60} and C_{70}[27−29] and found that M06-2X performs very well in understanding such reactions. The excellent performance of M06-2X functional originated from its introduction of dispersion corrections, which are essential for the theoretical investigation of fullerenes.[30] In the current project, using the same functional, we investigated the DA cycloadditions of CpH to $M^+@C_{60}$ (where M = Li, Na, K, Rb, and Cs) and $Ca^{2+}@C_{60}$ (Figure 1) in the gas phase and in a solvent. Via a discussion of the distortion and interaction energy model and comparison of the reaction with the empty C_{60}, the computational results uncover the fundamental role of encapsulated metal cations in the reactivity and regioselectivity of the C_{60} DA reaction. In the future, the mentioned DA reactions refer to the DA cycloadditions of CpH to C_{60}, $M^+@C_{60}$, and $Ca^{2+}@C_{60}$.

2. COMPUTATIONAL METHODS

All theoretical calculations were performed with the Gaussian 09 suite of programs.[31] Geometries of reactants (Rs), stable reactant complex (RCs), transition states (TSs), and products (Ps) were fully optimized using the M06-2X functional. A polarized double-ζ (6-31G(d,p)) basis set was used for C, H, Li, Na, and K atoms. The effective core potential-based LANL2DZ basis set was used for the heavy atoms Rb and Cs.[32,33] Harmonic vibrational frequencies were computed at the same theoretical level to verify the stationary points. Reaction path calculations were performed for all TSs to ensure that they connected the right local minimums. Zero-point vibrational energies (ZPVE) and thermal corrections at standard state (298 K and 1 atm) were also evaluated by the frequency calculations. The solvent effects of toluene (dielectric constant = 2.374) were modeled with the polarizable continuum model (PCM).[34] All the structures were reoptimized and then ZPVE and thermal corrections was obtained by frequency calculations in toluene at the same theoretical level as done under vacuum. The relative Gibbs energies of RCs and TSs to Rs and the reaction energy were denoted by ΔG_{RC}, ΔG_{TS}, and ΔG_r, respectively. The active barrier from RC to P was denoted by $\Delta G^{‡}$. The definitions of ΔG_{RC}, ΔG_{TS}, ΔG_r, and $\Delta G^{‡}$ are $\Delta G_{RC} = G_{RC} - (G_{R1} + G_{R2})$, $\Delta G_{TS} = G_{TS} - (G_{R1} + G_{R2})$, $\Delta G^{‡} = \Delta G^{TS} - \Delta G_{RC}$, and $\Delta G_r = G_p - (G_{R1} + G_{R2})$, where R1 denotes empty C_{60}, $M^+@C_{60}$, or $Ca^{2+}@C_{60}$ and R2 denotes CpH. The relative entropy and enthalpy values were defined in a similar way.

The distortion/interaction model divided the activation barrier into two imaginary categories: distortion energy and electronic interaction.[35−37] The distortion energy concerning the steric strain was unfavorable, whereas the electronic interaction was favorable to the cycloaddition reaction. Using the distortion/interaction model, Houk concluded that the reactivity of dienes is controlled by both distortion and interaction energies in the DA reactions of four cycloalkenes with four dienes.[38] Other

DOI: 10.1021/acs.jpca.5b00194
J. Phys. Chem. A 2015, 119, 3098−3106

Table 1. Dominant Geometric Parameters of Rs, RCs, TSs, and Ps in the DA Reactions of the Two Bonds of Empty C_{60}, $M^+@C_{60}$, and $Ca^{2+}@C_{60}$ as Well as the Only Imaginary Frequency of Each TS Calculated at the M06-2X/6-31G(d,p) Level of Theory under Vacuum (Units: Å for Bond Length and cm^{-1} for Frequency)

		RC					TS						P				
		r_i[a]	r_1[b]	r_2	r_5[c]	r_6	r_i	r_1	r_2	r_5	r_6	ν[c]	r_i	r_1	r_2	r_5	r_6
6−6 bond	empty C_{60}	1.387	NE[d]	NE	3.121	3.126	1.438	NE	NE	2.220	2.220	386i	1.603	NE	NE	1.584	1.584
	$Li^+@C_{60}$	1.397	2.277	2.279	2.994	2.995	1.453	2.335	2.334	2.220	2.221	324i	1.627	2.402	2.402	1.587	1.587
	$Na^+@C_{60}$	1.393	2.748	2.708	3.010	3.000	1.446	2.820	2.859	2.241	2.232	321i	1.611	3.071	3.071	1.588	1.588
	$K^+@C_{60}$	1.390	3.275	3.279	3.009	3.009	1.442	3.368	3.368	2.240	2.240	320i	1.606	3.641	3.641	1.588	1.588
	$Rb^+@C_{60}$	1.389	3.450	3.439	3.006	3.008	1.443	3.744	3.734	2.232	2.226	334i	1.605	3.983	3.944	1.588	1.588
	$Cs^+@C_{60}$	1.390	3.552	3.552	3.007	3.011	1.442	3.657	3.657	2.243	2.243	317*i*	1.607	3.873	3.874	1.588	1.588
	$Ca^{2+}@C_{60}$	1.402	2.687	2.687	2.761	2.762	1.453	2.736	2.736	2.303	2.304	185i	1.621	2.982	2.982	1.597	1.597
6−5 bond	empty C_{60}	1.451	NE	NE	3.318	3.318	1.504	NE	NE	2.103	2.104	572i	1.629	NE	NE	1.582	1.582
	$Li^+@C_{60}$	1.459	2.275	2.251	3.165	3.269	1.535	2.600	2.389	1.725	2.510	221i	1.651	2.442	2.442	1.586	1.586
	$Na^+@C_{60}$	1.456	2.713	2.788	3.156	3.255	1.529	3.336	3.419	1.720	2.549	214i	1.639	3.087	3.087	1.586	1.586
	$K^+@C_{60}$	1.453	3.288	3.274	3.188	3.276	1.526	3.723	3.638	1.732	2.252	229i	1.633	3.651	3.651	1.586	1.586
	$Rb^+@C_{60}$	1.453	3.448	3.461	3.243	3.302	1.526	3.731	3.584	1.733	2.251	230i	1.631	4.009	4.002	1.586	1.586
	$Cs^+@C_{60}$	1.454	3.546	3.541	3.225	3.293	1.527	3.803	3.620	1.734	2.550	228i	1.632	3.892	3.891	1.587	1.587
	$Ca^{2+}@C_{60}$	1.462	2.743	2.692	3.125	3.349	1.558	3.362	3.541	1.632	2.328	229i	1.650	2.985	2.985	1.598	1.598

[a] r_i is the distance between the two reactive carbon atoms, i.e., r_{ab} (6−6 bond) or r_{cd} (6−5 bond) in Figure 1, in empty C_{60}, $M^+@C_{60}$, and $Ca^{2+}@C_{60}$. [b] r_1 and r_2 are the distances between the metal cation and each of the two attacked carbon atoms, i.e., r_1 and r_2 in Figure 1 for 6−6 bond reactions. The r_2 data, i.e., the distances between the metal cations and carbon atom labeled c, were not shown in Figure 1. [c] r_5 and r_6 are the lengths of the two forming C−C bonds in the empty C_{60}, $M^+@C_{60}$, and $Ca^{2+}@C_{60}$ reactions; ν is the imaginary frequency of the saddle point; [d] No r_1 and r_2 data exist because there is no metal cation in empty C_{60}.

DOI: 10.1021/acs.jpca.5b00194
J. Phys. Chem. A 2015, 119, 3098−3106

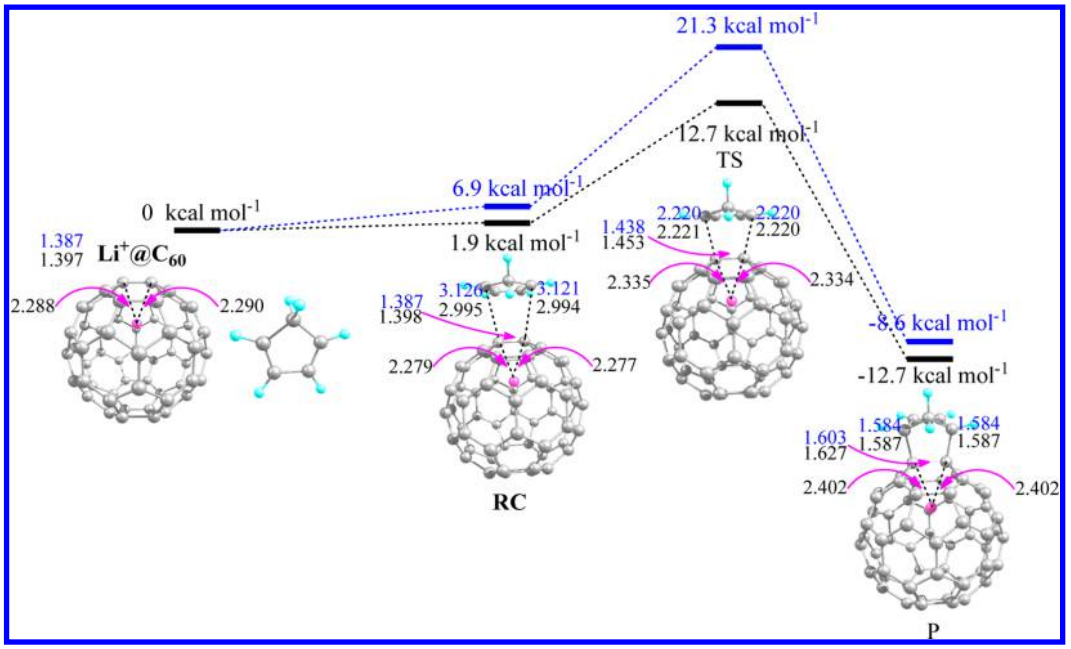

Figure 2. Reaction energy profiles (in Gibbs energy) and dominant structure parameters (in Å) of RCs, TSs, and Ps of the 6−6 bonds of empty C_{60} (blue) or $Li^+@C_{60}$ (black) calculated at the M06-2X/6-31G(d,p) level of theory. The distances between the Li^+ and the two attacked carbon atoms are also shown.

cycloaddition systems were also rationalized using this model.[39−44] The electronic activation barrier of the current DA cycloaddition reactions can be written as $\Delta E^{\ddagger} = \Delta E^{\ddagger}_{d1}$ (empty C_{60}, $M^+@C_{60}$, or $Ca^{2+}@C_{60}$) + $\Delta E^{\ddagger}_{d2}$ (CpH) + $\Delta E^{\ddagger}_{i}$, where $\Delta E^{\ddagger}_{d}$ represents the distortion energy, and $\Delta E^{\ddagger}_{i}$ represents the interaction energy. A similar model, the activation strain model,[45−50] was recently used for exploring the origin of the preference for the *endo* mode in the thermal DA cycloaddition of cyclopentadiene or butadiene to maleic anhydride along with the DA cycloaddition of *cis*-1,3-butadiene to $Ng_2@C_{60}$ (Ng = Ar, Kr, and Xe).[51,52] Combining both distortion/interaction and activation strain models, one can obtain a quantitative comprehension of the physical factors that control the activation energy through different fundamental processes.

3. RESULTS AND DISCUSSION

3.1. $M^+@C_{60}$ and $Ca^{2+}@C_{60}$. The dominant geometric parameters and the interaction energy in enthalpy and Gibbs energy are shown in Figure 1. Here, the interaction energy is defined as $\Delta E = E(M^+@C_{60}$ or $Ca^{2+}@C_{60}) - E(M^+$ or $Ca^{2+}) - E(C_{60})$, which is different from that in the distortion/interaction energy model. The Cartesian coordinates of the six EMCFs are listed in the Supporting Information. Dunlap demonstrated that in Li^+-, Na^+-, and K^+-encapsulated C_{60}, the equilibrium position of the alkali metal atom is at or very near the center of the C_{60} cage.[53] However, a first-principles study found that the encapsulated metal atoms are located away from the center of the C_{60} cage by approximately 1.403 Å for Li^+, 1.003 Å for Na^+, and 0.653 Å for K^+.[21] In Figure 1, it can be found that the distances between M^+ and carbon atoms a and b become larger moving down the periodic table. Li^+ and Na^+ are near the carbon edge, K^+ and Rb^+ are near the center, and Cs^+ is almost at the center of the C_{60} cage. X-ray diffraction indicated that Li^+ is located away from the center of the C_{60} cage by 1.340 Å.[3] Previous calculations showed that Na preferentially resides 1.030−1.060 Å from the center of the C_{60} cage in $Na@C_{60}$.[54] The current theoretical results suggest that Li^+, Na^+, K^+, and Ca^{2+} cations reside approximately 1.288, 0.817, 0.285, and 0.900 Å from the center, respectively, whereas Rb^+ and Cs^+ locate nearly at the center. The ionic radii of the cations increase in the following order: Li^+ (0.76 Å) < Na^+(1.02 Å) ≈ Ca^{2+}(1.00 Å) < K^+(1.38 Å) < Rb^+(1.52 Å) < Cs^+(1.67 Å).[55] Thus, we can conclude that the larger the cation radius, the nearer to the center of C_{60} cage that the cation lies.

The interactions between Li^+, Na^+, K^+, and Rb^+ ions and C_{60} are exothermic and exergonic; among them, the interaction between Li^+ and C_{60} is the strongest, whereas that between Rb^+ and C_{60} is the weakest. This is in accordance with a previous investigation.[53] The insertion of Cs^+ into the C_{60} cage is not a spontaneous process. The carbon−carbon bonds in five-membered or six-membered rings containing carbon atoms a or b change significantly to nearly the same extent, but the other carbon−carbon bonds change very little. Only the bond lengths of C_a−C_b (6−6 bond) and C_a−C_c (6−5 bond) are labeled in Figure 1. The following subsections are based on the DA cycloadditions of CpH to these two carbon bonds.

3.2. Geometric Changes. In the following discussion, for the aim of clarity, r_i is used to represent the distance between the two reactive carbon atoms, i.e., r_{ab} (6−6 bond) or r_{cd} (6−5 bond) in Figure 1; r_1 and r_2 are used to represent the distances between the metal cation and each of the two attacked carbon atoms, i.e., r_1 and r_2 in Figure 1 for 6−6 bond reactions; and r_5 and r_6 are used to represent the lengths of the two forming C−C bonds in all reactions. The dominant geometrical parameters of located stationary points as well as the only imaginary frequency of each TS are compiled in Table 1. The data of the reactions of the 6−6 bonds of empty C_{60} and $Li^+@C_{60}$ are depicted in Figure 2. We discuss the reaction process based on the 6−6 bond for the $Li^+@C_{60}$ reaction. A stable RC was located, as in our previous studies.[20,27,29] The distance between the two attacked carbon atoms remains nearly unchanged, and the two formed bonds are very long (2.994 and 2.995 Å). From R to RC to TS to P, r_5 and r_6 become shorter and shorter, whereas r_i, r_1, and r_2 become longer and longer accompanied by gradual changes in the C_a and C_b

DOI: 10.1021/acs.jpca.5b00194
J. Phys. Chem. A 2015, 119, 3098−3106

Table 2. ΔS, ΔH, and ΔG of the DA Reactions for the Two Types of Bonds in Empty C_{60}, $M^+@C_{60}$, and $Ca^+@C_{60}$ Calculated at the M06-2X/6-31G(d,p) Level of Theory under Vacuum (Units: kcal mol^{-1} for ΔH and ΔG and eu for ΔS, Where eu = cal·K^{-1}·mol^{-1})

		RC			TS			active barrier from RC			P		
		ΔS_{RC}	ΔH_{RC}	ΔG_{RC}	ΔS_{TS}	ΔH_{TS}	ΔG_{TS}	$\Delta S^{\ddagger}$	$\Delta H^{\ddagger}$	$\Delta G^{\ddagger}$	ΔS_r	ΔH_r	ΔG_r
6−6 bond	empty C_{60}	−39.2	−5.0	6.7	−47.0	7.3	21.3	−7.7	12.3	14.6	−51.7	−24.0	−8.6
	$Li^+@C_{60}$	−33.2	−8.0	1.9	−46.0	−1.0	12.7	−12.7	7.0	10.8	−52.3	−28.3	−12.7
	$Na^+@C_{60}$	−27.8	−7.2	1.1	−40.9	−0.4	11.8	−13.1	6.8	10.7	−46.0	−28.9	−15.2
	$K^+@C_{60}$	−37.9	−7.7	3.6	−48.3	−0.4	14.0	−10.4	7.3	10.4	−58.7	−30.0	−12.5
	$Rb^+@C_{60}$	−38.9	−6.4	5.2	−54.0	0.0	16.1	−15.1	6.4	10.9	−57.4	−28.5	−11.4
	$Cs^+@C_{60}$	−30.9	−5.7	3.5	−46.3	0.9	14.7	−15.4	6.6	11.2	−51.7	−28.1	−12.7
	$Ca^{2+}@C_{60}$	−58.0	−14.7	−2.6	−48.0	−13.8	0.5	−10.1	0.9	3.5	−53.7	−37.5	−21.5
6−5 bond	empty C_{60}	−36.9	−4.0	7.0	−46.0	23.1	36.8	−9.1	27.1	29.8	−51.3	−2.3	13.0
	$Li^+@C_{60}$	−41.6	−7.0	5.4	−49.6	11.9	26.7	−8.0	18.9	21.3	−48.3	−8.0	6.4
	$Na^+@C_{60}$	−37.6	−6.6	4.6	−42.9	13.0	25.8	−5.4	19.6	21.2	−51.3	−8.2	7.1
	$K^+@C_{60}$	−29.9	−5.7	3.2	−49.6	13.6	28.4	−19.8	19.3	25.2	−56.3	−8.2	8.6
	$Rb^+@C_{60}$	−41.6	−5.0	7.4	−50.0	14.8	29.7	−8.4	19.8	22.3	−52.7	−6.7	9.0
	$Cs^+@C_{60}$	−28.5	−3.7	4.8	−47.3	15.2	29.3	−18.8	18.9	24.5	−50.6	−5.9	9.2
	$Ca^{2+}@C_{60}$	−42.9	−11.9	0.9	−53.0	−4.9	10.9	−10.1	7.0	10.0	−51.7	−17.1	−1.7

hybridization from sp^2 to sp^3. The location of Li^+ in the C_{60} cage is not fixed. When CpH approaches $Li^+@C_{60}$, r_1 and r_2 change from 2.288 and 2.290 Å in R to 2.402 and 2.402 Å in P, respectively; thus, Li^+ moves toward the center of the fullerene cage as the reaction proceeds. The lengths of r_5 and r_6 in the six-membered-carbon-ring TS are nearly equal (2.220 and 2.221 Å), indicating that the reaction is a synchronous process. Both r_5 and r_6 in TS are nearly the same as those in the 6−6 bond of the empty C_{60} reaction. The other five 6−6 bond reactions have processes similar to that of the 6−6 bond in the $Li^+@C_{60}$ reaction, with the exception that r_5 and r_6 in the TS are all longer (earlier TSs) than those in the 6−6 bond of the empty C_{60} reaction.

The 6−5 bond of the $Li^+@C_{60}$ reaction is a bit surprising; the 6−5 bond reaction is no longer synchronous (r_5 and r_6 in the TS are very different), although the total reaction process is similar to that of the 6−6 bond reaction. The distances between Li^+ and the two attacked carbon atoms are different (r_1 and r_2 are 2.600 and 2.389 Å, respectively) in the TS. This indicates that as CpH approaches $Li^+@C_{60}$, Li^+ does not directly approach the center of C_{60} but moves a little closer to one of the two attacked atoms. This results in different reactivities for the two atoms. Thus, we think that the position of M^+ in $M^+@C_{60}$ or the TS more or less determines whether the DA reaction is synchronous or asynchronous. Interestingly, r_5 and r_6 are equal in all the 14 Ps, regardless of whether the TSs are the same. For the five $M^+@C_{60}$ reactions, r_5 and r_6 are all longer by nearly the same amount than those in the empty C_{60} reaction (0.003 Å for $Li^+@C_{60}$ and 0.004 Å for the other four $M^+@C_{60}$ 6−6 bond reactions, and 0.003 Å for $Cs^+@C_{60}$ and 0.004 Å for the other four $M^+@C_{60}$ 6−5 bond reactions). The lengths of r_5 and r_6 in $Ca^{2+}@C_{60}$ are the longest in both the 6−5 and 6−6 bond reactions. The Cartesian coordinates of all these stationary points are listed in the Supporting Information.

3.3. Thermodynamic Analysis. The thermochemical data are listed in Table 2. The relative Gibbs energies of the 6−6 bond for empty C_{60} and $Li^+@C_{60}$ reactions are depicted in Figure 2. The $\Delta H^{\ddagger}$(6−6) (6−6 in the parentheses indicates the data regarding the 6−6 bond reaction) of empty C_{60} is 12.3 kcal mol^{-1}, which is consistent with that calculated at the ONIOM2-(M06-2X/6-31G(d):SVWN/STO-3G) level of theory (12.1 kcal mol^{-1}).[30] The relatively low $\Delta H^{\ddagger}$ term is characteristic of concerted reactions, where the energy cost of bond breaking is compensated by the accompanying bond formation. The very negative entropy of the TS (ΔS_{TS}) reflects the loss of translational and rotational degrees of freedom in the formation of the highly ordered six-membered-ring TS. The ΔH_r is −24.0 kcal mol^{-1}, which is consistent with the results of Swart (−22.0 kcal mol^{-1}).[30] The experimental values of $\Delta H^{\ddagger}$ and ΔH_r are +6.9 and −19.8 ± 2.2 kcal mol^{-1}.[30,56,57] Compared to values for the empty C_{60} reaction, the ΔH and ΔG of the RCs and TSs are all lower for the $Li^+@C_{60}$ reactions. This indicates that the insertion of Li^+ stabilizes the RC and TS. The trivial differences between the relative entropies (ΔS) of the empty C_{60} and $Li^+@C_{60}$ reactions (Table 2) imply that the encapsulated cation does not significantly change the translational and rotational degrees of the reaction system. The $\Delta G^{\ddagger}$ for the $Li^+@C_{60}$ reaction is 10.8 kcal mol^{-1}, indicating that Li^+ catalyzed the reaction. The structural, chemical, and electronic properties of EMFs are different from those of empty fullerenes largely because of the electron transfer from the metal atom(s) to the carbon cage. The five metal cations other than Li^+ catalyze the empty C_{60} reaction via a similar mechanism. Na^+ catalyzed the reaction to nearly the same extent as Li^+, but the $Na^+@C_{60}$ reaction was more exergonic; thus, Na^+ may be a better catalyst than Li^+ for the DA of CpH to C_{60}. The sodium-encapsulated C_{60} was prepared recently.[54] We hope the current project can provide some motivation for the future investigation of the DA reaction of $Na@C_{60}$ and $Na^+@C_{60}$. The other three alkali metal cations do not enhance the reactivity compared to that of empty C_{60} more than Li^+ and Na^+. Similarly, it was demonstrated by B3LYP calculations that encapsulated Na^+ accelerates the DA cycloaddition of *cis*-1,3-butadiene to C_{32}, whereas encapsulated F^- does not.[58] Among all the targeted metal cations, Ca^{2+} exhibits the greatest catalytic ability; the RC, TS, and P are largely stabilized by Ca^{2+}, and the reaction barrier is the lowest.

The $\Delta G^{\ddagger}$(6−5) values for the $M^+@C_{60}$ reactions are also all lower than that of the empty C_{60} reaction. We suggest that M^+ ions promote the reactivity of both 6−6 and 6−5 bonds. The $\Delta G^{\ddagger}$(6−5) of empty C_{60} is 29.8 kcal mol^{-1}, which is 15.2 kcal mol^{-1} higher than that of the 6−6 bond reaction. The addition of CpH to empty C_{60} begins at the 6−6 bond from both the thermodynamic and kinetic viewpoints. This is in accordance with the experimental results for the DA cycloaddition of both CpH and 1,3-cyclohexadiene.[19,20] The differences between $\Delta G^{\ddagger}$(6−5) and $\Delta G^{\ddagger}$(6−6) are 15.2, 10.5, 10.5, 14.8, 8.8, 13.3,

DOI: 10.1021/acs.jpca.5b00194
J. Phys. Chem. A 2015, 119, 3098−3106

Table 3. $\Delta E^{\ddagger}$, $\Delta E_d^{\ddagger}$, and $\Delta E_i^{\ddagger}$ of the DA Reactions of the Two Types of Bonds in Empty C_{60}, $M^+@C_{60}$, and $Ca^+@C_{60}$ Calculated at the M06-2X/6-31G(d,p) Level of Theory under Vacuum (kcal mol^{-1})[a]

		total $\Delta E_d^{\ddagger}$	$\Delta E_{d1}^{\ddagger}$		$\Delta E_{d2}^{\ddagger}$		$\Delta E_i^{\ddagger}$	$\Delta E^{\ddagger}$
6−6 bond	empty C_{60}	20.0	6.1	31%	13.9	70%	−7.6	12.4
	$Li^+@C_{60}$	19.4	6.4	33%	13.0	67%	−11.7	7.7
	$Na^+@C_{60}$	18.6	6.1	33%	12.5	67%	−11.1	7.5
	$K^+@C_{60}$	18.3	5.8	32%	12.5	68%	−11.1	7.2
	$Rb^+@C_{60}$	19.4	6.3	32%	13.1	68%	−11.4	8.0
	$Cs^+@C_{60}$	18.3	5.9	32%	12.4	68%	−11.2	7.1
	$Ca^{2+}@C_{60}$	13.2	4.6	35%	8.6	65%	−11.9	1.3
6−5 bond	empty C_{60}	33.3	12.0	36%	21.3	64%	−5.9	27.4
	$Li^+@C_{60}$	43.8	18.5	42%	25.3	58%	−25.3	18.5
	$Na^+@C_{60}$	43.7	18.5	42%	25.2	58%	−24.4	19.3
	$K^+@C_{60}$	42.1	17.6	42%	24.5	58%	−21.8	20.3
	$Rb^+@C_{60}$	42.0	17.6	42%	24.4	58%	−22.0	20.0
	$Cs^+@C_{60}$	42.6	18.1	42%	24.5	58%	−22.8	19.8
	$Ca^{2+}@C_{60}$	61.5	25.4	41%	36.1	59%	−55.1	6.2

[a] $\Delta E_{d1}^{\ddagger}$ is the distortion energy of empty C_{60}, $M^+@C_{60}$ or $Ca^{2+}@C_{60}$, $\Delta E_{d2}^{\ddagger}$ is the distortion energy of CpH, and $\Delta E_i^{\ddagger}$ is the interaction energy in each DA cycloaddition reaction. The percentages of $\Delta E_{d1}^{\ddagger}$ and $\Delta E_{d2}^{\ddagger}$ in $\Delta E_d^{\ddagger}$ are also included.

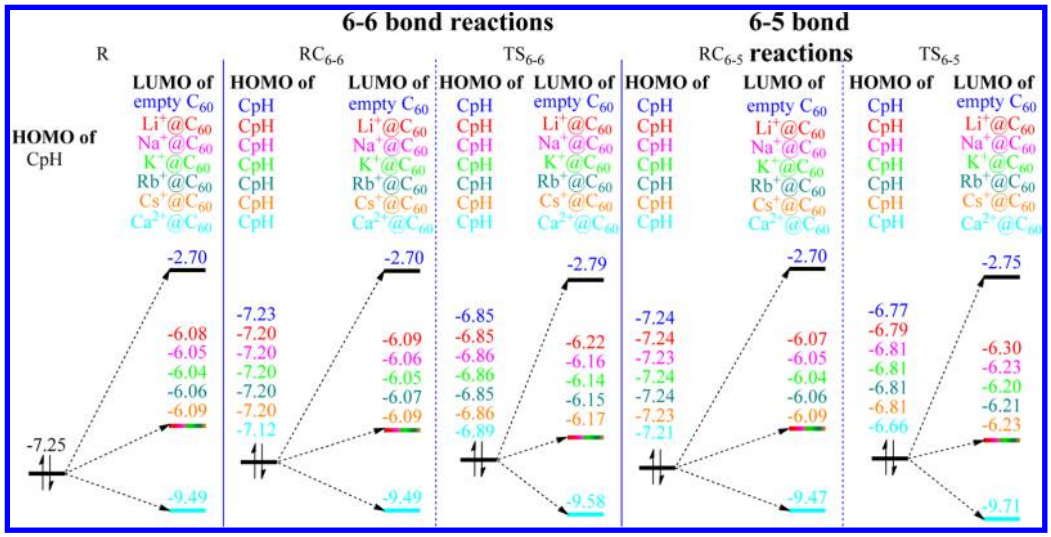

Figure 3. Energies (eV) of CpH HOMOs and empty C_{60}, $M^+@C_{60}$, and $Ca^{2+}@C_{60}$ LUMOs along with those of the distorted forms in RCs and TSs calculated at the M06-2X/6-31G(d,p) level of theory under vacuum.

and 6.5 kcal mol^{-1} for empty C_{60}, $Li^+@C_{60}$, $Na^+@C_{60}$, $K^+@C_{60}$, $Rb^+@C_{60}$, $Cs^+@C_{60}$, and $Ca^{2+}@C_{60}$, respectively. Thus, first, although the reactivities of the 6−5 bonds in $M^+@C_{60}$ and $Ca^{2+}@C_{60}$ are increased, they are still lower than those of the 6−6 bonds. Second, it can be found that the $\Delta G^{\ddagger}$(6−5) of Ca^{2+} is similar to the $\Delta G^{\ddagger}$(6−6) values of the five $M^+@C_{60}$, the reaction is very exergonic (negative ΔG_r), which suggests that the reactivity of the 6−5 bond in $Ca^{2+}@C_{60}$ is high. In conclusion, the difference between the 6−6 and 6−5 bond reactivities becomes smaller when more positive charges are introduced into the C_{60} cage. This gives a practicable way to electrochemically control of the regioselectivity of the exohedral functionalization of C_{60}.[59]

3.4. Distortion/Interaction and Frontier Molecular Orbital (FMO) Analysis. The distortion and interaction energies are listed in Table 3. The distortion energies are the electronic energies of the fragments in the TSs relative to those in the RCs as there is some noncovalent interaction between the two reactants in the RCs. The distortion energies are 6.1 and 13.9 kcal mol^{-1} for empty C_{60} and CpH in the 6−6 bond reaction, respectively. The distortion of CpH is dominant, accounting for 70% of the total distortion energy. In total, 20.0 kcal mol^{-1} is needed for the two reactants to distort to their structures to the TS. The distorted reactants interact more easily, decreasing the activation barrier by 7.6 kcal mol^{-1}, and the final barrier is 12.4 kcal mol^{-1}. After Li^+ is encapsulated in the C_{60} cage, $\Delta E_d^{\ddagger}$ is slightly decreased by 0.6 kcal mol^{-1}, but the interactions between the two distorted reactants in the TS increase by 4.1 kcal mol^{-1}. The final activation barrier decreases by 4.7 kcal mol^{-1}. The other four alkali metal cations affect the distortion and interaction energies of the empty C_{60} reaction to similar extents. For the $Ca^{2+}@C_{60}$ reaction, the lengths of r_5 (2.303 Å) and r_6 (2.304 Å) are longer than those of $M^+@C_{60}$, indicating an earlier TS. This results in a total distortion energy of 13.2 kcal mol^{-1}, which is 6.8 and 5.1−6.2 kcal mol^{-1} smaller than those of the empty C_{60} and $M^+@C_{60}$ reactions, respectively. Although the interaction energy is similar to those of the $M^+@C_{60}$ reactions, the final barrier is very low.

For the 6−5 bond reaction in empty C_{60}, the total distortion energy is higher by 13.3 kcal mol^{-1}, and the interaction is lower by 1.7 kcal mol^{-1} compared to that of the 6−6 bond reaction. The higher distortion energy corresponds to the later TS of the

DOI: 10.1021/acs.jpca.5b00194
J. Phys. Chem. A 2015, 119, 3098−3106

Table 4. ΔS, ΔH, and ΔG of the DA Cycloadditions of CpH to the Two Types of Bonds of Empty C_{60}, $M^+@C_{60}$, and $Ca^{2+}@C_{60}$ Calculated at the M06-2X/6-31G(d,p) Level of Theory in Toluene (Units: kcal mol^{-1} for ΔH and ΔG and eu for ΔS, Where eu = $cal{\cdot}K^{-1}{\cdot}mol^{-1}$)

		RC			TS			active barrier from RC			P		
		ΔS_{RC}	ΔH_{RC}	ΔG_{RC}	ΔS_{TS}	ΔH_{TS}	ΔG_{TS}	$\Delta S^{\ddagger}$	$\Delta H^{\ddagger}$	$\Delta G^{\ddagger}$	ΔS_r	ΔH_r	ΔG_r
6−6 bond	empty C_{60}	−38.9	−4.0	7.6	−47.0	7.6	21.6	−8.0	11.6	14.0	−51.7	−23.4	−8.0
	$Li^+@C_{60}$	−43.9	−7.0	6.1	−47.0	1.0	15.0	−3.0	8.0	8.9	−51.0	−26.4	−11.2
	$Na^+@C_{60}$	−29.2	−5.5	3.2	−44.3	1.4	14.6	−15.1	6.9	11.4	−51.0	−27.4	−12.2
	$K^+@C_{60}$	−33.9	−5.8	4.3	−50.0	0.9	15.8	−16.1	6.7	11.5	−63.7	−29.1	−10.1
	$Rb^+@C_{60}$	−32.2	−4.4	5.2	−41.3	2.9	15.2	−9.1	7.3	10.0	−45.6	−26.4	−12.8
	$Cs^+@C_{60}$	−32.9	−5.0	4.8	−46.3	2.3	16.1	−13.4	7.3	11.3	−51.7	−26.6	−11.2
	$Ca^{2+}@C_{60}$	−41.3	−9.9	2.4	−53.3	−10.4	5.5	−12.1	−0.5	3.1	−58.0	−33.9	−16.6
6−5 bond	empty C_{60}	−28.2	−2.7	5.7	−45.3	23.4	36.9	−17.1	26.1	31.2	−51.3	−1.7	13.6
	$Li^+@C_{60}$	−32.5	−3.9	5.8	−48.3	14.1	28.5	−15.8	18.0	22.7	−49.3	−5.1	9.6
	$Na^+@C_{60}$	−43.3	−5.8	7.1	−46.6	14.8	28.7	−3.4	20.6	21.6	−51.3	−6.2	9.1
	$K^+@C_{60}$	−35.2	−4.7	5.8	−51.7	14.4	29.8	−16.4	19.1	24.0	−58.0	−6.8	10.5
	$Rb^+@C_{60}$	−43.6	−4.1	8.9	−44.9	16.4	29.8	−1.3	20.5	20.9	−45.6	−4.5	9.1
	$Cs^+@C_{60}$	−41.3	−3.6	8.7	−48.3	16.0	30.4	−7.0	19.6	21.7	−50.6	−4.5	10.6
	$Ca^{2+}@C_{60}$	−35.2	−7.8	2.7	−56.7	−0.4	16.5	−21.5	7.4	13.8	−52.3	−11.8	3.8

6−5 bond reaction (r_1 is 2.103 Å and r_2 is 2.104 Å) compared to that for the 6−6 bond reaction (r_1 and r_2 are both 2.220 Å). The final electronic activation barrier is 27.4 kcal mol^{-1}, which is much higher than that of the 6−6 bond reaction. The larger distortion energy indicates a higher reaction barrier. For the 6−5 bond reaction of each $M^+@C_{60}$, the total distortion energy is much larger than that of the corresponding 6−6 bond reaction. This finding is easily understood because the deformation of $M^+@C_{60}$ is larger for the asynchronous process of the 6−5 bond reaction. However, the interaction energy is even higher for $M^+@C_{60}$, which makes the final activation energy lower for $M^+@C_{60}$ than that of the empty C_{60}. The DA reaction on $Ca^{2+}@C_{60}$ deserves more discussion. Its distortion energy is the largest among the 6−5 bond reactions, but the smallest among the 6−6 bond reactions of the six systems (Table 3). The TS (r_5 is 1.632 Å and r_6 is 2.328 Å) of the 6−5 bond reaction of $Ca^{2+}@C_{60}$ is the latest one among all the studied encapsulated cation reactions, which leads to the large distortion. The highest interaction energy of this 6−5 reaction (Table 3) resulted from the more adapted FMOs of the reactants. The combined distortion and interaction resulted in a low activation barrier (6.2 kcal mol^{-1}), which is much lower than those of the other reactions. Although the reactivity of the 6−5 bond reaction is still lower than the 6−6 one for $Ca^{2+}@C_{60}$, as in the other $M^+@C_{60}$, the difference between the activation energies of the reactions of the two bonds is much smaller for $Ca^{2+}@C_{60}$ (4.9 kcal mol^{-1}) than for the other $M^+@C_{60}$ (11−13 kcal mol^{-1}). This means that the encapsulation of cations with more positive charges can change the regioselectivity because these charges change the aromaticity of the five- and six-membered rings of C_{60}. A previous study concluded that as the number of electrons added to the C_{60} cage increases from C_{60}^- to C_{60}^{6-}, the DA regioselectivity changes from the usual 6−6 bond to the 6−5 bond.[59]

The difference in interaction can be understood on the basis of the electronic structure change during the distortion process. In Figure 3, the HOMOs of CpH and LUMOs of empty C_{60}, $M^+@C_{60}$, and $Ca^{2+}@C_{60}$ along with those of the distorted forms in the RCs and TSs are depicted. The detailed FMO data are listed in Table S1 (Supporting Information). It can be found that the gap between HOMO of CpH and LUMOs of empty C_{60}, $M^+@C_{60}$, and $Ca^{2+}@C_{60}$ in 6−6 bond reactions are all narrower than the one in the corresponding 6−5 bond reactions. This makes 6−6 bond reactions more favorable, which is in accordance with the previous study.[50] Both the HOMOs and LUMOs of $M^+@C_{60}$ and $Ca^{2+}@C_{60}$ are stabilized to nearly the same extent compared to those of empty C_{60}, which is consistent with the experimental results.[13] In the reaction of CpH and the 6−6 bond of empty C_{60}, the CpH HOMO changes from −7.25 to −7.23 to −6.85 eV, and the empty C_{60} LUMO changes from −2.70 to −2.70 to −2.79 eV. This tendency can be described as follows. From R to RC to TS, the CpH HOMO become higher, while the C_{60} and $M^+@C_{60}$ LUMOs become lower; thus, the gap between them becomes narrower, facilitating their interaction. The $M^+@C_{60}$ LUMOs are largely lower than that of empty C_{60}, so the gaps between them and the corresponding CpH HOMOs are much narrower than the gaps in the empty C_{60} reactions. The inserted M^+ facilitate the interaction between CpH and C_{60}. The gaps between the CpH HOMO and each $M^+@C_{60}$ LUMO are similar; thus, the interaction energies are also similar. Especially, the $Ca^{2+}@C_{60}$ LUMO lies below the CpH HOMO, indicating that the interaction between them occurs the easiest.

3.5. Solvent Effects. In our previous studies, the DA reactions of empty C_{60} were not significantly influenced by both polar and nonpolar solvents.[27,29] In the present study, the charges on $M^+@C_{60}$ and $Ca^{2+}@C_{60}$ are relatively dispersed to CpH, which may be slightly favored by a nonpolar solvent. The DA cycloaddition of CpH to $Li^+@C_{60}$[19] was explored in toluene. The calculated results are collected in Table 4. The dominant parameters of the optimized geometries of all the stationary points in toluene are listed in Table S2 (Supporting Information). The effects of toluene on the structures of all the stationary points are small for the 12 studied reactions. For the two empty C_{60} reactions, the relative entropies and Gibbs energies of the RCs, TSs, and Ps are all within 1 kcal mol^{-1}. The $\Delta G^{\ddagger}$ for the DA cycloaddition of CpH to the 6−6 bond of $Li^+@C_{60}$ is lower by nearly 2.0 kcal mol^{-1}. The 6−6 bond reaction of $Ca^{2+}@C_{60}$ is also promoted by toluene. The other reactions are slightly promoted by toluene.

4. CONCLUSION

The DA cycloadditions of CpH to the 6−6 and 6−5 bonds of empty C_{60}, $M^+@C_{60}$, and $Ca^{2+}@C_{60}$ were systematically investigated at the M06-2X/6-31G(d,p) theoretical level. On the basis of the calculated results, the relative reactivities of the

DOI: 10.1021/acs.jpca.5b00194
J. Phys. Chem. A 2015, 119, 3098−3106

two types of bonds were compared. The promotion ability of the encapsulated alkali metal cations and Ca^{2+} were understood from different angles. The results were in line with previous theoretical computations and experimental observations. The main conclusions of the current project were collected as follows: (i) for isolated $M^+@C_{60}$ and $Ca^{2+}@C_{60}$ molecules, the positions of the metal cations inside the C_{60} cages were different; (ii) the interactions between metal cations and C_{60} are exothermic and exergonic, with the exception of Cs^+; (iii) 6−6 bond reactions are concerted and synchronous processes, whereas all 6−5 bond reactions are concerted and asynchronous processes; (iv) metal cations can promote the reactions of CpH and C_{60} because they decrease the activation barriers and make the reactions more exothermic and exergonic or less endothermic and endergonic; (v) Na^+ has relatively strong catalytic ability among $M^+@C_{60}$, and the DA cycloaddition of CpH to $Ca^{2+}@C_{60}$ occurs more easily than all the five $M^+@C_{60}$; (vi) encapsulated cations change both the distortion and interaction energies, and the combined effect facilitates the DA reactions of the cation-encapsulated C_{60} molecules; (vii) the HOMO−LUMO gap becomes smaller as the reaction proceeds, which facilitates interaction between the distorted reactants; (viii) the activation barrier in solvent is similar to that under vacuum for all reactions, but the reaction heat is more favorable for $M^+@C_{60}$ forward reactions; (ix) encapsulated metal cations with more positive charges enhance the reactivity of the 6−5 bond in C_{60}, which is significant when the 6−5 adduct is the target product.

■ ASSOCIATED CONTENT

Supporting Information

The Cartesian coordinates of optimized structures, the detailed FMO data, the dominant parameters of the optimized geometries of all the stationary points in toluene have been collected in the Supporting Information. Full ref 31. This material is available free of charge via the Internet at http://pubs.acs.org/.

■ AUTHOR INFORMATION

Corresponding Author

*Y.-J. Liu. E-mail: yajun.liu@bnu.edu.cn.

Notes

The authors declare no competing financial interest.

■ ACKNOWLEDGMENTS

This study was supported by grants from the National Nature Science Foundation of China (Grant Nos. 21273021, 21325312, and 21421003) and the Major State Basic Research Development Programs (Grant No. 2011CB808500).

■ REFERENCES

(1) Whitehouse, D. B.; Buckingham, A. D. The Vibrational Contribution to the Polarisability of Endohedral $[C_{60}M]^{n+}$ Complexes (Where M = Metal Atom). *Chem. Phys. Lett.* **1993**, *207*, 332−338.

(2) Tellgmann, R.; Krawez, N.; Lin, S. H.; Hertel, I. V.; Campbell, E. E. B. Endohedral Fullerene Production. *Nature* **1996**, *382*, 407−408.

(3) Aoyagi, S.; Nishibori, E.; Sawa, H.; Sugimoto, K.; Takata, M.; Miyata, Y.; Kitaura, R.; Shinohara, H.; Okada, H.; Sakai, T.; et al. A Layered Ionic Crystal of Polar $Li@C_{60}$ Superatoms. *Nat. Chem.* **2010**, *2*, 678−683.

(4) Fukuzumi, S.; Ohkubo, K.; Kawashima, Y.; Kim, D. S.; Park, J. S.; Jana, A.; Lynch, V. M.; Kim, D.; Sessler, J. L. Ion-Controlled On−Off Switch of Electron Transfer from Tetrathiafulvalene Calix[4]Pyrroles to $Li^+@C_{60}$. *J. Am. Chem. Soc.* **2011**, *133*, 15938−15941.

(5) Heath, J. R.; O'Brien, S. C.; Zhang, Q.; Liu, Y.; Curl, R. F.; Tittel, F. K.; Smalley, R. E. Lanthanum Complexes of Spheroidal Carbon Shells. *J. Am. Chem. Soc.* **1985**, *107*, 7779−7780.

(6) Popov, A. A.; Yang, S.; Dunsch, L. Endohedral Fullerenes. *Chem. Rev.* **2013**, *113*, 5989−6113.

(7) Kubozono, Y.; Ohta, T.; Hayashibara, T.; Maeda, H.; Ishida, H.; Kashino, S.; Oshima, K.; Yamazaki, H.; Ukita, S.; Sogabe, T. Preparation and Extraction of $Ca@C_{60}$. *Chem. Lett.* **1995**, *24*, 457−458.

(8) Kubozono, Y.; Maeda, H.; Takabayashi, Y.; Hiraoka, K.; Nakai, T.; Kashino, S.; Emura, S.; Ukita, S.; Sogabe, T. Extractions of $Y@C_{60}$, $Ba@C_{60}$, $La@C_{60}$, $Ce@C_{60}$, $Pr@C_{60}$, $Nd@C_{60}$, and $Gd@C_{60}$ with Aniline. *J. Am. Chem. Soc.* **1996**, *118*, 6998−6999.

(9) Sidorov, N. S.; Palnichenko, A. V.; Rybchenko, O. G.; Khasanov, S. S. Intercalation of C_{60} Fullerene Crystals with Calcium and Barium via Self-Propagating High-Temperature Synthesis. *Inorg. Mater.* **2010**, *46*, 476−479.

(10) Sidorov, N. S.; Palnichenko, A. V.; Rybchenko, O. G.; Khasanov, S. S.; Vyaselev, O. M. A Technique for the Rapid Intercalation of Alkali and Alkaline-Earth Metals into Crystalline C_{60} Using Self-Propagating High Temperature Synthesis. *Carbon* **2009**, *47*, 3019−3022.

(11) Hebard, A. F.; Rosseinsky, M. J.; Haddon, R. C.; Murphy, D. W.; Glarum, S. H.; Palstra, T. T. M.; Ramirez, A. P.; Kortan, A. R. Superconductivity at 18 K in Potassium-Doped C_{60}. *Nature* **1991**, *350*, 600−601.

(12) Haddon, R. C.; Hebard, A. F.; Rosseinsky, M. J.; Murphy, D. W.; Duclos, S. J.; Lyons, K. B.; Miller, B.; Rosamilia, J. M.; Fleming, R. M.; Kortan, A. R.; et al. Conducting Films of C_{60} and C_{70} by Alkali-Metal Doping. *Nature* **1991**, *350*, 320−322.

(13) Okada, H.; Komuro, T.; Sakai, T.; Matsuo, Y.; Ono, Y.; Omote, K.; Yokoo, K.; Kawachi, K.; Kasama, Y.; Ono, S.; et al. Preparation of Endohedral Fullerene Containing Lithium ($Li@C_{60}$) and Isolation as Pure Hexafluorophosphate Salt ($[Li^+@C_{60}][PF_6^-]$). *RSC Adv.* **2012**, *2*, 10624−10631.

(14) Ueno, H.; Kokubo, K.; Kwon, E.; Nakamura, Y.; Ikuma, N.; Oshima, T. Synthesis of a New Class of Fullerene Derivative $Li^+@C_{60}O(OH)_7$ as a "Cation-Encapsulated Anion Nanoparticle". *Nanoscale* **2013**, *5*, 2317−2321.

(15) Matsuo, Y.; Okada, H.; Maruyama, M.; Sato, H.; Tobita, H.; Ono, Y.; Omote, K.; Kawachi, K.; Kasama, Y. Covalently Chemical Modification of Lithium Ion-Encapsulated Fullerene: Synthesis and Characterization of $[Li^+@PCBM]PF_6^-$. *Org. Lett.* **2012**, *14*, 3784−3787.

(16) Ohkubo, K.; Kawashima, Y.; Fukuzumi, S. Strong Supramolecular Binding of $Li^+@C_{60}$ with Sulfonated Meso-Tetraphenylporphyrins and Long-Lived Photoinduced Charge Separation. *Chem. Commun.* **2012**, *48*, 4314−4316.

(17) Kawashima, Y.; Ohkubo, K.; Fukuzumi, S. Efficient Charge Separation in $Li^+@C_{60}$ Supramolecular Complexes with Electron Donors. *Chem.—Asian J.* **2015**, *10*, 44−54.

(18) Osuna, S.; Swart, M.; Sola, M. The Reactivity of Endohedral Fullerenes. What Can Be Learnt from Computational Studies? *Phys. Chem. Chem. Phys.* **2011**, *13*, 3585−3603.

(19) Kawakami, H.; Okada, H.; Matsuo, Y. Efficient Diels−Alder Addition of Cyclopentadiene to Lithium Ion Encapsulated [60]-Fullerene. *Org. Lett.* **2013**, *15*, 4466−4469.

(20) Ueno, H.; Kawakami, H.; Nakagawa, K.; Okada, H.; Ikuma, N.; Aoyagi, S.; Kokubo, K.; Matsuo, Y.; Oshima, T. Kinetic Study of the Diels−Alder Reaction of $Li^+@C_{60}$ with Cyclohexadiene: Greatly Increased Reaction Rate by Encapsulated Li^+. *J. Am. Chem. Soc.* **2014**, *136*, 11162−11167.

(21) Noguchi, Y.; Sugino, O.; Okada, H.; Matsuo, Y. First-Principles Investigation on Structural and Optical Properties of $M^+@C_{60}$ (Where M = H, Li, Na, and K). *J. Phys. Chem. C* **2013**, *117*, 15362−15368.

(22) Zhao, Y.; Truhlar, D. The M06 Suite of Density Functionals for Main Group Thermochemistry, Thermochemical Kinetics, Noncovalent Interactions, Excited States, and Transition Elements: Two New Functionals and Systematic Testing of Four M06-Class Functionals and 12 Other Functionals. *Theor. Chem. Acc.* **2008**, *120*, 215−241.

DOI: 10.1021/acs.jpca.5b00194
J. Phys. Chem. A 2015, 119, 3098−3106

(23) Pieniazek, S. N.; Clemente, F. R.; Houk, K. N. Sources of Error in DFT Computations of C-C Bond Formation Thermochemistries: $\pi \rightarrow \sigma$ Transformations and Error Cancellation by DFT Methods. *Angew. Chem.* **2008**, *120*, 7860−7863.
(24) Sato, S.; Maeda, Y.; Guo, J.-D.; Yamada, M.; Mizorogi, N.; Nagase, S.; Akasaka, T. Mechanistic Study of the Diels−Alder Reaction of Paramagnetic Endohedral Metallofullerene: Reaction of La@C_{82} with 1,2,3,4,5-Pentamethylcyclopentadiene. *J. Am. Chem. Soc.* **2013**, *135*, 5582−5587.
(25) Paton, R. S.; Mackey, J. L.; Kim, W. H.; Lee, J. H.; Danishefsky, S. J.; Houk, K. N. Origins of Stereoselectivity in the Trans Diels−Alder Paradigm. *J. Am. Chem. Soc.* **2010**, *132*, 9335−9340.
(26) Lan, Y.; Zou, L.; Cao, Y.; Houk, K. N. Computational Methods to Calculate Accurate Activation and Reaction Energies of 1,3-Dipolar Cycloadditions of 24 1,3-Dipoles. *J. Phys. Chem. A* **2011**, *115*, 13906−13920.
(27) Gao, X.-F.; Cui, C.-X.; Liu, Y.-J. Trapping Intermediates and Comparing Relative Reactivities: A DFT M06-2X Study on Diels−Alder Cycloadditions of Butadiene to C_{60} and C_{70}. *J. Phys. Org. Chem.* **2012**, *25*, 850−855.
(28) Cui, C.-X.; Liu, Y.-J. A Thorough Understanding of the Diels−Alder Reaction of 1,3-Butadiene and Ethylene. *J. Phys. Org. Chem.* **2014**, *27*, 652−660.
(29) Cui, C.-X.; Liu, Y.-J. A Theoretical Study of the Mechanisms for 1,3-Dipolar Cycloadditions of Diphenyldiazomethane to C_{60} and C_{70}. *J. Phys. Org. Chem.* **2014**, *27*, 823−832.
(30) Osuna, S. l.; Swart, M.; Solà, M. Dispersion Corrections Essential for the Study of Chemical Reactivity in Fullerenes. *J. Phys. Chem. A* **2011**, *115*,, 3491−3496.
(31) Frisch, M.; Trucks, G.; Schlegel, H.; Scuseria, G.; Robb, M.; Cheeseman, J.; Scalmani, G.; Barone, V.; Mennucci, B.; Petersson, G. *Gaussian 09*, Revision A.02; Gaussian Inc.: Wallingford, CT, 2009.
(32) Ghatee, M. H.; Niroomand-Hosseini, F. Contribution of Dispersive Second Virial Coefficient of Liquid Cesium Metal. *J. Phys. Chem. B* **2004**, *108*, 10034−10040.
(33) Zhang, Y.; Wang, X.; Luo, B.; Xia, Y. DFT Study of Crown Ether-Bridged Z-Stilbenes and Their Complexes with Alkali Metal Cations. *J. Organomet. Chem.* **2012**, *699*, 31−38.
(34) Tomasi, J.; Persico, M. Molecular Interactions in Solution: An Overview of Methods Based on Continuous Distributions of the Solvent. *Chem. Rev.* **1994**, *94*, 2027−2094.
(35) Ess, D. H.; Houk, K. N. Distortion/Interaction Energy Control of 1,3-Dipolar Cycloaddition Reactivity. *J. Am. Chem. Soc.* **2007**, *129*, 10646−10647.
(36) Lan, Y.; Houk, K. N. Mechanism and Stereoselectivity of the Stepwise 1,3-Dipolar Cycloadditions between a Thiocarbonyl Ylide and Electron-Deficient Dipolarophiles: A Computational Investigation. *J. Am. Chem. Soc.* **2010**, *132*, 17921−17927.
(37) Liu, S.; Lei, Y.; Qi, X.; Lan, Y. Reactivity for the Diels−Alder Reaction of Cumulenes: A Distortion-Interaction Analysis Along the Reaction Pathway. *J. Phys. Chem. A* **2014**, *118*, 2638−2645.
(38) Liu, F.; Paton, R. S.; Kim, S.; Liang, Y.; Houk, K. N. Diels−Alder Reactivities of Strained and Unstrained Cycloalkenes with Normal and Inverse-Electron-Demand Dienes: Activation Barriers and Distortion/Interaction Analysis. *J. Am. Chem. Soc.* **2013**, *135*, 15642−15649.
(39) Domingo, L. R.; Saez, J. A.; Joule, J. A.; Rhyman, L.; Ramasami, P. A Dft Study of the [3 + 2] Versus [4 + 2] Cycloaddition Reactions of 1,5,6-Trimethylpyrazinium-3-Olate with Methyl Methacrylate. *J. Org. Chem.* **2013**, *78*, 1621−1629.
(40) Gordon, C. G.; Mackey, J. L.; Jewett, J. C.; Sletten, E. M.; Houk, K. N.; Bertozzi, C. R. Reactivity of Biarylazacyclooctynones in Copper-Free Click Chemistry. *J. Am. Chem. Soc.* **2012**, *134*, 9199−9208.
(41) Knall, A. C.; Slugovc, C. Inverse Electron Demand Diels-Alder (iEDDA)-Initiated Conjugation: A (High) Potential Click Chemistry Scheme. *Chem. Soc. Rev.* **2013**, *42*, 5131−5142.
(42) Liang, Y.; Mackey, J. L.; Lopez, S. A.; Liu, F.; Houk, K. N. Control and Design of Mutual Orthogonality in Bioorthogonal Cycloadditions. *J. Am. Chem. Soc.* **2012**, *134*, 17904−17907.
(43) Lopez, S. A.; Munk, M. E.; Houk, K. N. Mechanisms and Transition States of 1,3-Dipolar Cycloadditions of Phenyl Azide with Enamines: A Computational Analysis. *J. Org. Chem.* **2013**, *78*, 1576−1582.
(44) Schoenebeck, F.; Houk, K. N. Ligand-Controlled Regioselectivity in Palladium-Catalyzed Cross Coupling Reactions. *J. Am. Chem. Soc.* **2010**, *132*, 2496−2497.
(45) Bickelhaupt, F. M. Understanding Reactivity with Kohn−Sham Molecular Orbital Theory: E2−S_N2 Mechanistic Spectrum and Other Concepts. *J. Comput. Chem.* **1999**, *20*, 114−128.
(46) de Jong, G. T.; Bickelhaupt, F. M. Transition-State Energy and Position Along the Reaction Coordinate in an Extended Activation Strain Model. *ChemPhysChem* **2007**, *8*, 1170−1181.
(47) Diefenbach, A.; Bickelhaupt, F. M. Oxidative Addition of Pd to C−H, C−C and C−Cl Bonds: Importance of Relativistic Effects in DFT Calculations. *J. Chem. Phys.* **2001**, *115*, 4030−4040.
(48) Diefenbach, A.; de Jong, G. T.; Bickelhaupt, F. M. Activation of H−H, C−H, C−C and C−Cl Bonds by Pd and $PdCl^-$. Understanding Anion Assistance in C−X Bond Activation. *J. Chem. Theory Comput.* **2005**, *1*, 286−298.
(49) van Zeist, W.-J.; Bickelhaupt, F. M. The Activation Strain Model of Chemical Reactivity. *Org. Biomol. Chem.* **2010**, *8*, 3118−3127.
(50) Fernández, I.; Solà, M.; Bickelhaupt, F. M. Why Do Cycloaddition Reactions Involving C60 Prefer [6,6] over [5,6] Bonds? *Chem.—Eur. J.* **2013**, *19*, 7416−7422.
(51) Fernández, I.; Solà, M.; Bickelhaupt, F. M. Origin of Reactivity Trends of Noble Gas Endohedral Fullerenes Ng_2@C_{60} (Ng = He to Xe). *J. Chem. Theory Comput.* **2014**, *10*, 3863−3870.
(52) Fernández, I.; Bickelhaupt, F. M. Origin of the "Endo Rule" in Diels−Alder Reactions. *J. Comput. Chem.* **2014**, *35*, 371−376.
(53) Dunlap, B. I.; Ballester, J. L.; Schmidt, P. P. Interactions between C-60 and Endohedral Alkali Atoms. *J. Phys. Chem.* **1992**, *96*, 9781−9787.
(54) Dunk, P. W.; Adjizian, J. J.; Kaiser, N. K.; Quinn, J. P.; Blakney, G. T.; Ewels, C. P.; Marshall, A. G.; Kroto, H. W. Metallofullerene and Fullerene Formation from Condensing Carbon Gas under Conditions of Stellar Outflows and Implication to Stardust. *Proc. Natl. Acad. Sci. U. S. A.* **2013**, *110*, 18081−18086.
(55) Shannon, R. D. Revised Effective Ionic Radii and Systematic Studies of Interatomic Distances in Halides and Chalcogenides. *Acta. Crystallogr. A* **1976**, *32*, 751−767.
(56) Pang, L. S. K.; Wilson, M. A. Reactions of Fullerenes C_{60} and C_{70} with Cyclopentadiene. *J. Phys. Chem.* **1993**, *97*, 6761−6763.
(57) Barco, J. W.; Yadav, T.; Lafleur, A. L.; Marr, J. A.; Howard, J. B.; Rotello, V. M. Kinetic Stability of the Fullerene C_{60}-Cyclopentadiene Diels-Alder Adduct. *J. Phys. Chem.* **1993**, *97*, 8560−8561.
(58) Ravinder, P.; Subramanian, V. Role of Encapsulation of Na^+ and F^- Ions on the Diels−Alder Reactivity of C_{32}. *J. Phys. Chem. A* **2012**, *116*, 6870−6878.
(59) Garcia-Borras, M.; Osuna, S.; Swart, M.; Luis, J. M.; Sola, M. Electrochemical Control of the Regioselectivity in the Exohedral Functionalization of C_{60}: The Role of Aromaticity. *Chem. Commun.* **2013**, *49*, 1220−1222.

DOI: 10.1021/acs.jpca.5b00194
J. Phys. Chem. A 2015, 119, 3098−3106